PROCEEDINGS OF SCIENCE

Electroweak and QCD aspects in V+jets in CMS

Stephane Cooperstein, on behalf of the CMS Collaboration*
University of California San Diego
E-mail: stephane.b.cooperstein@cern.ch

The study of the associated production of vector bosons and jets constitutes an excellent test-bench to check numerous QCD predictions. The most recent measurements of total and differential cross sections of vector bosons produced in association with jets are presented. Differential distributions as function of a broad range of kinematical observables are measured and compared with theoretical predictions. Final states with a vector boson and jets can be also used to study electroweak-initiated processes, such as the vector boson fusion production of a Z or W boson that are accompanied by a pair of energetic jets with large invariant mass. The study of these processes enables quantitative assessment of the reliability of the generator predictions for vector boson fusion topologies as well as stringent constraints on anomalous triple gauge coupling effective field theory parameters.

European Physical Society Conference on High Energy Physics - EPS-HEP2019 -
10-17 July, 2019
Ghent, Belgium

*Speaker.

PoS(EPS-HEP2019)670

1. Introduction

The study of the associated production of vector bosons and jets (V+jets) is an important precision test of QCD predictions. Moreover, V+jets processes are a major background in a large variety of analyses at the LHC ranging from searches for supersymmetry to precision measurements of the Higgs boson. Figure 1 shows the theory prediction and measured cross sections by CMS [1] for Standard Model (SM) processes at LHC center-of-mass energies. V+jets events, shown in the first two columns of Figure 1, are one of the primary processes produced in LHC pp collisions. Understanding V+jets processes with high precision is therefore fundamental to the LHC physics program. The unprecendented scale of the available V+jets dataset furthermore enables extremely high precision tests of QCD predictions.

A small subset of inclusive V+jets events are electroweak-initiated. These electroweak (EW) Vjj processes are an important probe of vector boson fusion (VBF) processes, which exhibit a distinct signature of two quark jets with large dijet invariant mass and large jet pseudorapidity separation. The measurement of EW Vjj processes is essential in validating the modeling of other important VBF processes such as VBF Higgs boson production, and furthermore provides strong constrains on anomalous triple gauge coupling effective field theory (EFT) parameters.

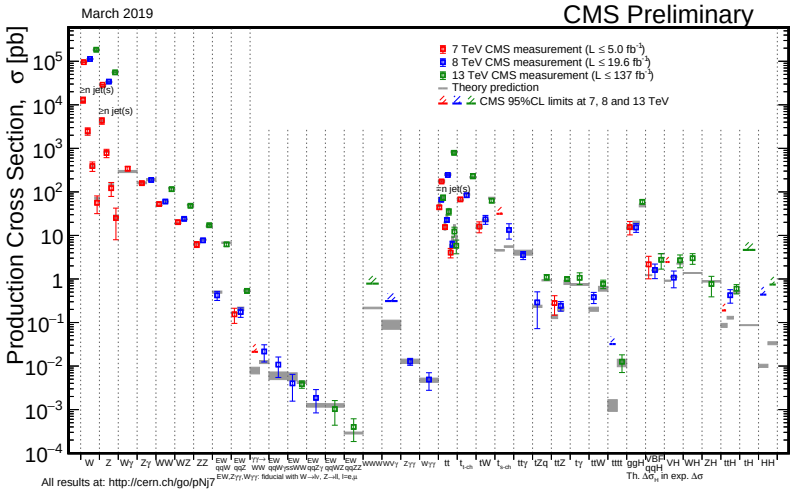

Figure 1: Summary of CMS measurements of SM processes, compared to theoretical predictions [1].

2. W+jets at 13 TeV

W+jets events are selected by requiring one muon with $p_T > 25$ GeV and $|\eta| < 2.4$. The neutrino momentum transverse to the beam line is assumed to be the event transverse momentum imbalance. The transverse mass of the W boson candidate is required to be at least 50 GeV. Events are then categorized based on the jet multiplicity, where the jets considered have $p_T > 30$ GeV and $|\eta| < 2.4$. The primary background is from $t\bar{t}$, with a relative contamination fraction increasing with jet multiplicity. The subdominant background from QCD multijet is estimated via a data-driven method.

An iterative d'Agostini unfolding is performed for the jet kinematic observables in order to compare the generator-level predictions with 2.2 fb^{-1} of $\sqrt{s} = 13$ TeV data. Figure 2 shows the leading jet p_T and the jet H_T distributions for events with at least three jets. The data are compared with the leading order (up to four jets) and next-to-leading order (up to two jets) MADGRAPH5 amc@NLO predictions as well as a fixed order calculation at next-to-next-to-leading order (NNLO) with one jet. Good agreement is observed between the predictions and data, although the leading order (LO) prediction slightly underestimates the data for the low-p_T observables [2].

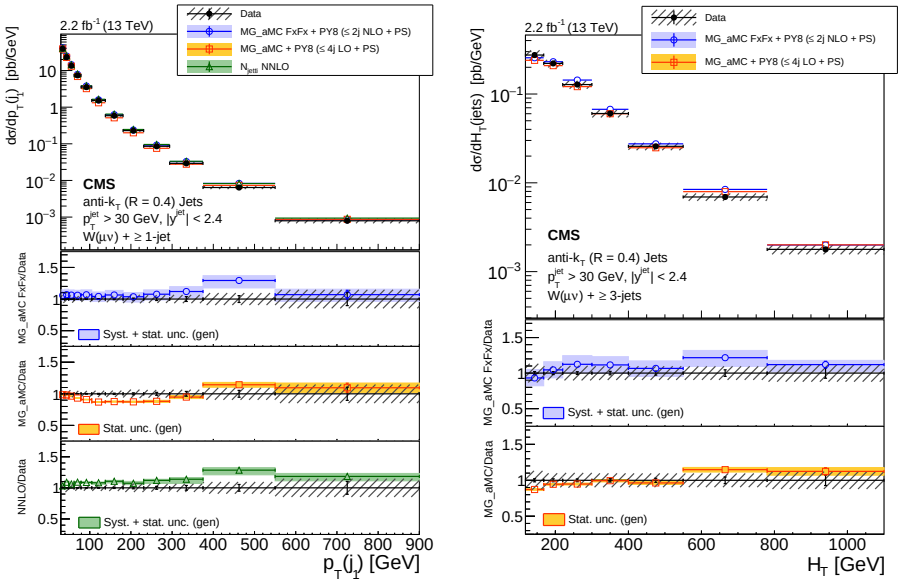

Figure 2: Unfolded leading jet p_T (left) and jet H_T for W+jets events with at least three jets (right) [2].

3. Z+jets at 13 TeV

A high-purity Z+jets sample is obtained by selecting events with two opposite-sign electrons or muons with $p_T > 20$ GeV, $|\eta| < 2.4$, and dilepton invariant mass within 20 GeV of the Z boson mass. Events are then categorized based on the jet multiplicity, where the jets considered have $p_T > 30$ GeV and $|\eta| < 2.4$. An iterative d'Agostini unfolding is performed, with the $Z \to \tau\tau$ contribution subtracted, to compare generator predictions with 2.2 fb^{-1} of $\sqrt{s} = 13$ TeV data [3]. Figure 3 shows the event p_T balance (left) and Z boson p_T (right) distributions for events with at least one jet. The data are compared with the LO (up to four jets) and next-to-leading order (up to two jets) MADGRAPH5 amc@NLO predictions as well as a fixed order calculation at NNLO with one jet and a calculation with GENEVA at NNLO with next-to-next-to-leading log (NNLL) resummation. The NLO predictions agree well with the data, whereas significant discrepancies are observed between the data and the LO predictions for the jet kinematic observables. The event p_T balance, sensitive to additional hadronic activity, is not well described by the NNLO + NNLL prediction.

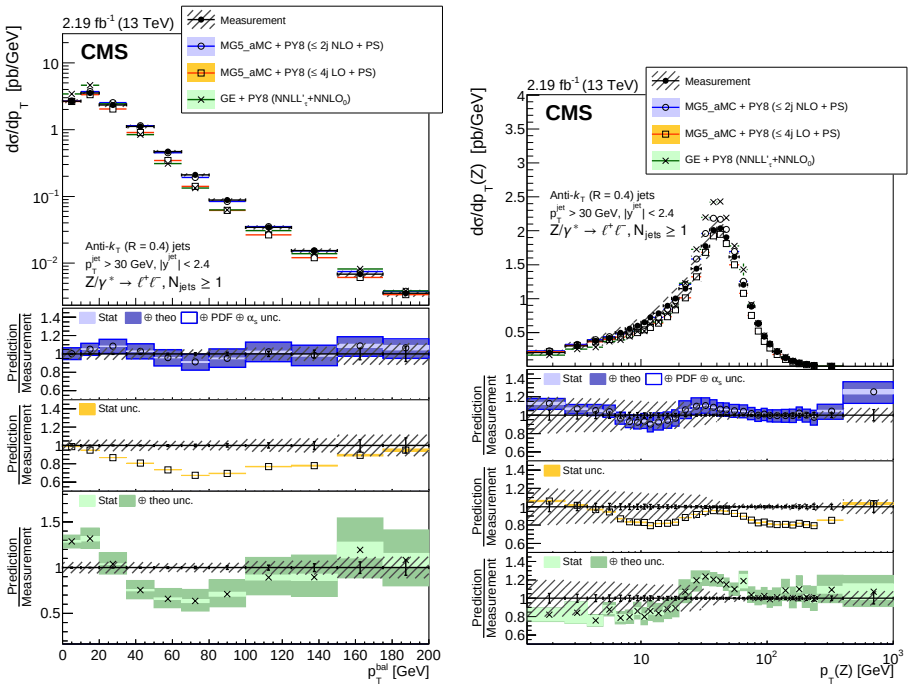

Figure 3: Unfolded event p_T balance (left) and Z boson p_T (right) distributions compared to data, for Z+jets events with at least one jet [3].

4. Electroweak Zjj

Electroweak-initiated Z+jets (EW Zjj) events provide an excellent probe of VBF topologies. The EW Zjj process is furthermore an important background in the measurement of VBF Higgs boson production. The EW Zjj signal is defined as the $\ell\ell$jj final state with $m_{jj} > 120$ GeV, $p_{T,j} > 25$ GeV, and $m(\ell\ell) > 50$ GeV. The dominant background is from Drell-Yan, with additional small contamination from top and diboson events as well as interference between the EW Zjj signal and the QCD-initiated Z+jets background.

A boosted decision tree (BDT) is trained to separate the EW Zjj signal from the Drell-Yan background. The primary discriminating BDT input observable is the m_{jj}, with the relative EW Zjj fraction steadily increasing with increasing m_{jj}. Figure 4 shows the distribution of the BDT score for the selected dielectron (left) and dimuon (right) events. A binned maximum-likelihood fit is performed on the BDT score to extract the EW Zjj signal, resulting in a measured cross section of

$$\sigma(\text{EW } \ell\ell\text{jj}) = 552 \pm 0.19(\text{stat.}) \pm 55(\text{syst.})\text{fb}, \tag{4.1}$$

in good agreement with the leading order SM prediction [4]. The measurement is dominated by systematic uncertainties, with the largest contribution from the experimental uncertainty on the jet energy scale.

For the electroweak-initiated signal, a suppression of hadronic activity is expected in the rapidity gap between the two quark jets. A tight selection on the BDT score is applied in order to obtain a region with similar yields in signal and background. In this highly VBF-enriched region,

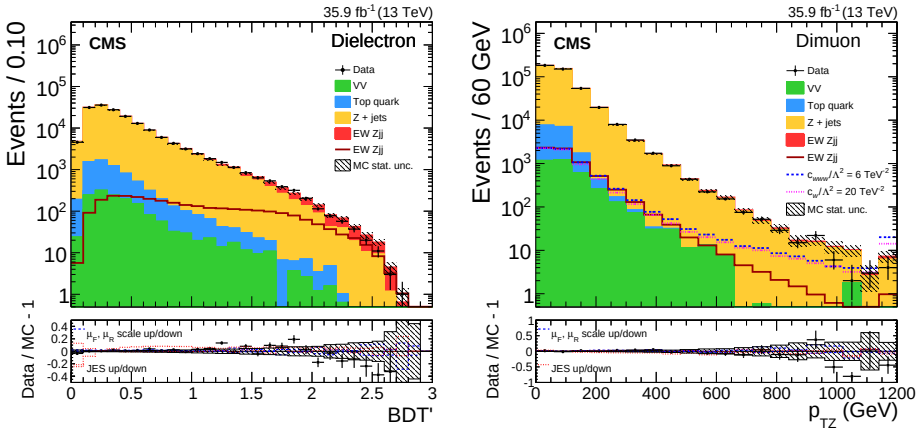

Figure 4: EW Zjj BDT score for dielectron (left) and dimuon (right) selected events [4].

additional physical observables probing the hadronic activity in the jet rapidity gap are considered. The comparison of these distributions in data with the prediction from simulation probes directly the parton shower modeling. For this study, rapidity gap "soft activity" track-only observables are included that allow probing of very low in p_T without large pileup jet contamination.

Figure 5 shows the total H_T of track-only soft activity jets in the rapidity gap in the selected region with BDT score greater than 0.92. The data are compared to the leading order signal prediction plus PYTHIA8 (left) and HERWIG++ (right) parton shower. Figure 6 shows the efficiency of an event veto on hadronic activity in the rapidity gap as a function of the leading jet p_T (left) and the track-only jet H_T (right). The data are compared with the background-only prediction as well as the background plus signal prediction, where the leading order signal is interfaced with either PYTHIA or HERWIG parton shower. The data at low gap activity values tend to prefer the prediction from the HERWIG.

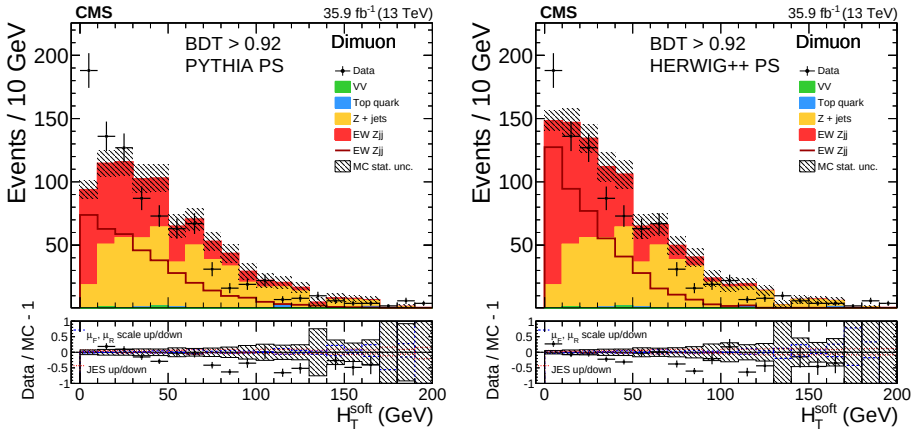

Figure 5: Total H_T of track-only soft activity jets in the rapidity gap between the two quarks jets for EW Zjj-enriched events with BDT score greater than 0.92, with the signal prediction at leading order plus PYTHIA8 (left) and HERWIG++ (right) parton shower [5].

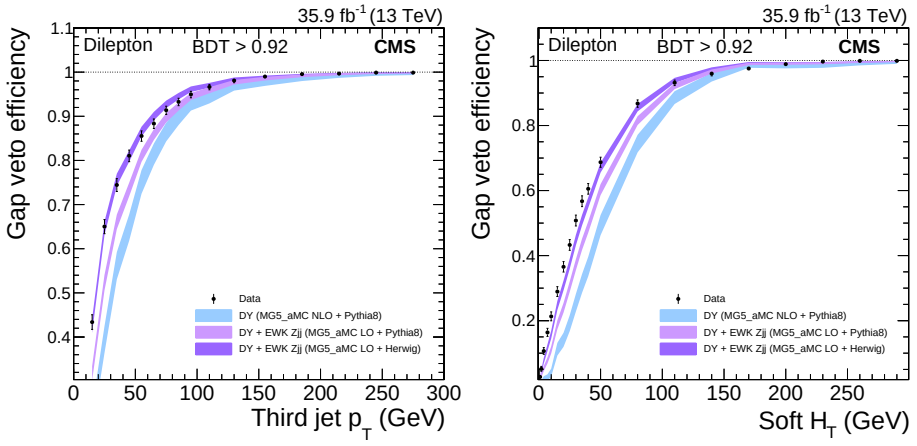

Figure 6: Gap activity veto efficiency as a function of the leading jet p_T (left) and the track-only jet H_T (right) in a high-purity EW Zjj data sample [4].

5. Electroweak Wjj

The measurement of the EW Wjj process is more experimentally challenging than EW Zjj due to the missing energy from the neutrino from the W boson decay and significant background contributions from QCD multijet and top events in addition to W+jets. The selected region is very similar to the EW Zjj measurement, plus additional selections to reduce the QCD multijet and top backgrounds. Despite the additional challenges in measuring the EW Wjj, the relatively large cross section of this process allows probing of VBF topologies with an order of magnitude greater statistics in data than for the EW Zjj.

The EW Wjj signal is extracted via a binned maximum-likelihood fit on the output of a BDT trained to discriminate the EW Wjj signal from the W+jets background. Figure 7 shows the BDT score after the fit in the muon (left) and electron (right) channels. The measured EW Wjj cross section is

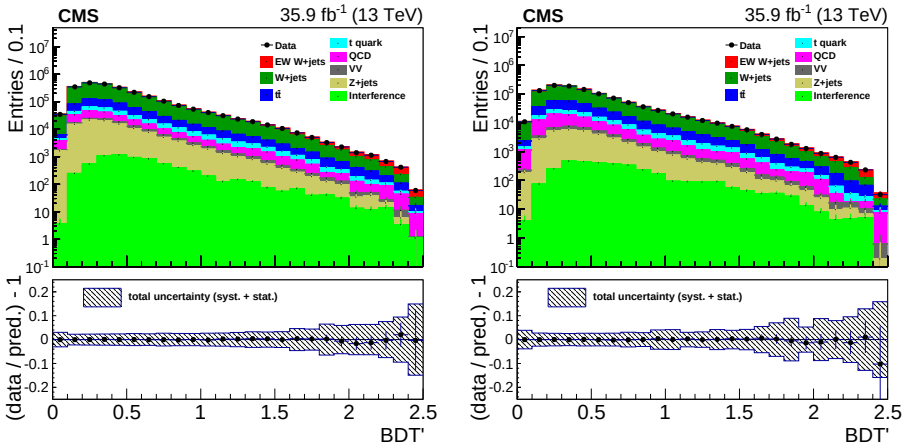

Figure 7: EW Wjj BDT score for the muon (left) and electron (right) channel selected events [5].

$$\sigma(\text{EW } \ell\ell\text{jj}) = 6.23 \pm 0.12(\text{stat.}) \pm 0.61(\text{syst.})\text{pb}, \tag{5.1}$$

in good agreement with the leading order SM prediction [5]. The rapidity gap acitivity veto efficiency is studied in a highly VBF-enriched region with BDT score greater than 0.95 in order to quantatively assess the reliability of the parton shower modeling in VBF topologies. Figure 8 shows the gap activity veto efficiency as a function of the leading jet p_T (left) and the leading track-only jet p_T (right). The result is well compatible with the equivalent study of the EW Zjj-enriched region described in the previous section, with the data prefering the HERWIG++ parton shower prediction over PYTHIA8 at low gap activity. The high statistics in data of the EW Wjj sample allows for fine probing of gap activity down to several GeV. At these very low gap activity thresholds, the data is observed to be even softer than the HERWIG prediction.

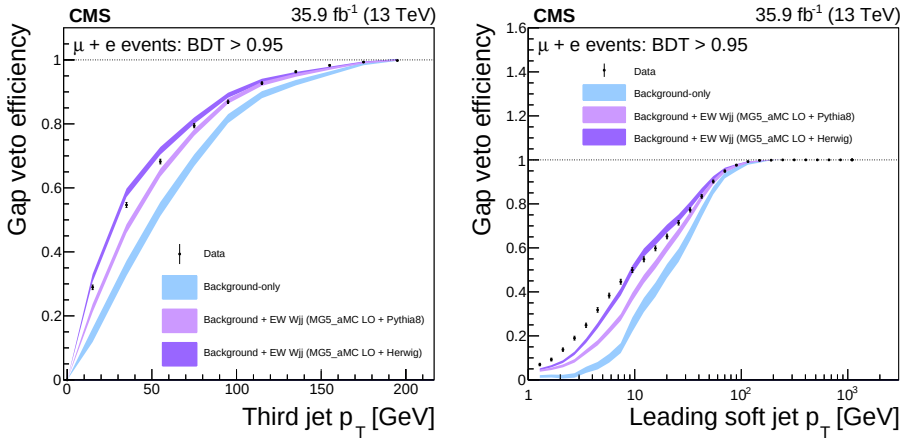

Figure 8: Gap activity veto efficiency as a function of the leading jet p_T (left) and the leading track-only jet p_T (right) in a high-purity EW Wjj data sample [5].

6. Anomalous triple gauge couplings

Deviations from the SM can be parametrized in terms of an effective field theory (EFT) framework in which beyond the SM interactions at a large energy scale Λ would manifest as small deviations of the coefficients of SM operators at LHC collision energies. The EW Zjj and EW Wjj processes give direct access to the WWZ and WWγ vertices. Measuring the high-energy tails of kinematic distributions for these processes therefore enables strong constraints on anomalous tiple gauge coupling (ATGC) EFT parameters.

A simultaneous binned maximum-likelihood fit is performed on the $p_T(Z)$ in the EW Zjj region and the lepton p_T for EW Wjj events. The sensitivity to ATGC parameters has been improved by 20-25% in the EW Wjj analysis by including an optimized selection on the BDT score. Figure 9 shows the fitted distributions, while Table 1 summarizes the observed constraints on the ATGC EFT parameters.

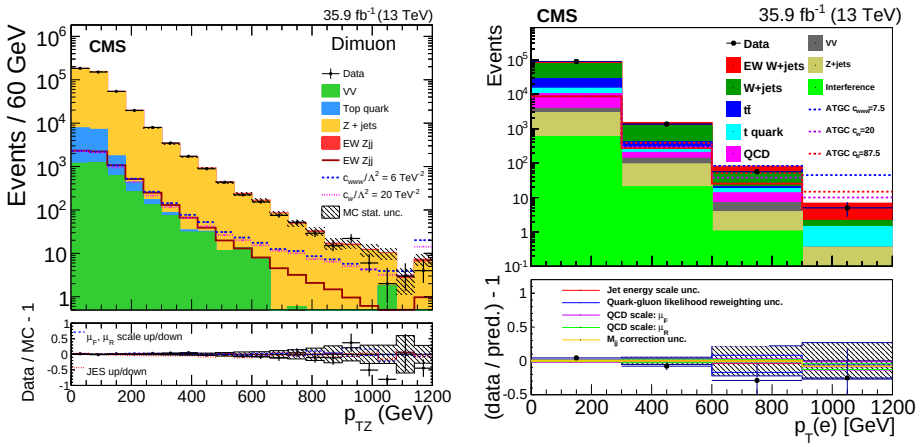

Figure 9: $p_T(Z)$ for EW Zjj (left) and p_T for EW Wjj selected events (right) [4, 5].

Table 1: One-dimensional limits on the ATGC EFT parameters at 95% CL from the combination of EW Wjj and EW Zjj analyses [5].

Coupling constant	Expected 95% CL interval (TeV^{-2})	Observed 95% CL interval (TeV^{-2})
c_{WWW}/Λ^2	$[-2.3, 2.4]$	$[-1.8, 2.0]$
c_W/Λ^2	$[-11, 14]$	$[-5.8, 10.0]$
c_B/Λ^2	$[-61, 61]$	$[-43, 45]$

7. Conclusion

The study of V+jets, one of the primary processes in LHC collisions, provides a stringent test of QCD predictions and is essential to understand with precision for a large variety of measurements and searches. Both the W+jets and Z+jets processes have been measured by CMS with 2.3 fb^{-1} of $\sqrt{s} = 13$ TeV data, with extensive comparisons of unfolded data with the prediction from multiple generators at LO and NLO, as well as NNLO fixed order calculations. CMS has also performed dedicated measurements of the electroweak-initiated Zjj and Wjj processes with 35.9 fb^{-1} of $\sqrt{s} = 13$ TeV data. These measurements allow for a quantative assessment of the reliability of generator predictions for VBF topologies and enable stringent constraints on anomalous triple gauge coupling EFT parameters.

References

[1] CMS Collaboration, *JINST* **3**, S08004 (2008).

[2] CMS Collaboration, *Phys. Rev.* D **96**, 072005 (2017).

[3] CMS Collaboration, *Eur. Phys. J.* C **78**, 965 (2018).

[4] CMS Collaboration, *Eur. Phys. J.* C **78**, 589 (2018).

[5] CMS Collaboration, Submitted to *Eur. Phys. J.* C(2019): arXiv:1903.04040.